Proximal and Distal Effects on the Coordination Chemistry of Ferric *Scapharca* Homodimeric Hemoglobin As Revealed by Heme Pocket Mutants†

Alberto Boffi,* Laura Guarrera, Laura Giangiacomo, Carla Spagnuolo, and Emilia Chiancone

Consiglio Nazionale della Ricerche Center of Molecular Biology, Department of Biochemical Sciences, University "La Sapienza", 00185 Rome, Italy

Received October 4, 1999; Revised Manuscript Received January 3, 2000

ABSTRACT: The ferric form of the homodimeric hemoglobin from *Scapharca inaequivalvis* (HbI) displays a unique pH-dependent behavior involving the interconversion among a monomeric low-spin hemichrome, a dimeric high-spin aquomet six-coordinate derivative, and a dimeric high-spin five-coordinate species that prevail at acidic, neutral, and alkaline pH values, respectively. In the five-coordinate derivative, the iron atom is bound to a hydroxyl group on the distal side since the proximal Fe−histidine bond is broken, possibly due to the packing strain exerted by the Phe97 residue on the imidazole ring [Das, T. K., Boffi, A., Chiancone, E. and Rousseau, D. L. (1999) *J. Biol. Chem*. *274*, 2916−2919]. To determine the proximal and distal effects on the coordination and spin state of the iron atom and on the association state, two heme pocket mutants have been investigated by means of optical absorption, resonance Raman spectroscopy, and analytical ultracentrifugation. Mutation of the distal histidine to an apolar valine causes dramatic changes in the coordination and spin state of the iron atom that lead to the formation of a five-coordinate derivative, in which the proximal Fe−histidine bond is retained, at acidic pH values and a high-spin, hydroxyl-bound six-coordinate derivative at neutral and alkaline pH values. At variance with native HbI, the His69 → Val mutant is always high-spin and does not undergo dissociation into monomers at acidic pH values. The Phe97 → Leu mutant, like the native protein, forms a monomeric hemichrome species at acidic pH values. However, at alkaline pH, it does not give rise to the unusual hydroxyl-bound five-coordinate derivative but forms a six-coordinate derivative with the proximal His and distal hydroxyl as iron ligands.

Ferric hemoglobins and myoglobins are frequently used as models for the study of the structural and functional properties of the physiologically active ferrous derivatives.[1] Ferric hemoproteins are amenable to a number of spectroscopic investigations that are sensitive to specific stereochemical features of the heme iron environment due to the multiplicity of the ferric iron spin states. Such sensitivity may offer a detailed insight into the finer structural adjustments of the heme iron that lead to the tuning of the protein function. Thus, hemoproteins in the ferric state often represent the system of choice for the study of heme reactivity toward charged ligands (*2*) as well as for investigations on the spin properties of the iron atom in response to conformational perturbations (*3*). The assignment of both the coordination state and the nature of the bound ligand in the sixth coordination position is a prerequisite for such studies.

Ferric *Scapharca inaequivalvis* homodimeric hemoglobin (HbI) has been extensively investigated due to its unique pH-linked coordination and spin state equilibria. In a first report, sedimentation velocity, optical absorption, and electron paramagnetic resonance (EPR) experiments demonstrated that HbI undergoes a complex pH-dependent equilibrium in which dimeric high-spin species, which predominate at neutral and alkaline pH values, dissociate reversibly into a low-spin monomeric species upon acidification (*4*). The coordination states of low-spin and high-spin species of ferric HbI have been assigned subsequently by means of resonance Raman, optical absorption, and EPR spectroscopy (*5*, *6*). Thus, ferric HbI can be described in the framework of an equilibrium among three distinct species, a dimeric pentacoordinate derivative that dominates the experimental situation at pH values above 7.0, a dimeric aquomet species that is present in sizable amounts around neutrality, and a monomeric hemichrome that is formed at acidic pH values. The nature of the low-spin hexacoordinate hemichrome species was inferred by similarity of the EPR spectrum with that of distorted bis-histidine ferric heme (*7*). It was suggested that the distal His (H69) provides the sixth iron coordination ligand. More recently, the fifth ligand in the pentacoordinate species was found to be a hydroxyl group that binds the heme iron from the distal side of the heme pocket by means of resonance Raman experiments (*1*). This surprising result is at variance with the proximal-histidine ferric pentacoordinate species found in several myoglobin mutants (*1*, *8*, *9*). The unusual coordination geometry of the *Scapharca* pentacoordinate derivative has been further confirmed by comparison with heme model compounds in micellar systems

* Corresponding author: Fax 39-6-444 0062; Email Boffi@axrma.uniroma1.it.

† This work was supported in part by MURST grants 60% and "Biologia Strutturale" to E.C.

[1] Abbreviations: HbI, *Scapharca inaequivalvis* homodimeric hemoglobin; Phe97 → Leu HbI, dimeric *Scapharca inaequivalvis* hemoglobin mutant in position Phe97 → Leu; His69 → Val HbI, dimeric *Scapharca inaequivalvis* hemoglobin mutant in position His69 → Val.

10.1021/bi9923003 CCC: $19.00
Published on Web 03/03/2000

and the relevant spectral properties fully assessed (*10*). However, the structural constraints that are at the basis of the unexpected coordination geometry in HbI have not been unveiled.

Inspection of the crystallographic structures of liganded and unliganded ferrous HbI derivatives has shown that the iron coordination state is tuned by the movement of the Phe97 residue, which is tightly packed against the proximal histidine in the ligand-bound derivative and is displaced from the heme pocket to the intersubunit interface in the deoxy pentacoordinate derivative. The movement of Phe97, therefore, is a major component of the transfer of information between the two hemes, i.e., of the cooperative behavior in HbI (*11*−*13*). In this framework, a relevant question concerns the role of Phe97 in determining the iron coordination state in the ferric derivative. It is not clear whether the stabilization of the pentacoordinate hydroxyl-bound derivative results from Phe97 being in a deoxy "T-like" or in an oxy "R-like" position. To clarify this point and, in addition, gain information on the conformational changes in the heme pocket that lead to the stabilization of the hemichrome species, we investigated the pH-dependent spectroscopic properties of two heme pocket mutants. The study of the Phe97 → Leu mutant is relevant to understand the structural constraints on the proximal side that lead to the stabilization of the hydroxyl-bound pentacoordinate species, while the analysis of the distal histidine mutant His69 → Val provides information on the effect of a decreased polarity of the distal pocket on the coordination chemistry of the iron and permits the definitive assignment of the sixth ligand in the monomeric hemichrome species.

MATERIALS AND METHODS

The homodimeric hemoglobin (HbI) from the mollusc *S. inaequivalvis* was extracted and purified as previously described (*14*). The protein concentration is expressed on a heme basis and was determined at 578 nm in the oxy state and at 556 nm in the deoxy state using the molar extinction coefficients $\epsilon = 14\ 300\ M^{-1}\ cm^{-1}$ and $\epsilon = 12\ 000\ M^{-1}\ cm^{-1}$, respectively (*14*). The single mutation His69 → Val was obtained as described in Guarrera et al. (*15*). The single mutation Phe97 → Leu was obtained as described in Pardanani et al. (*16*). Expression of the mutants in *Escherichia coli* and protein purification were carried out as described for recombinant wild-type HbI (*17*).

Oxidation was obtained by addition of potassium ferricyanide in slight molar excess to solutions of hemoglobin at pH 7.0 in 0.1 M phosphate buffer. The excess of oxidant was removed by passage on a Sephadex G-25 column equilibrated with the desired buffer.

Spectrophotometric pH titrations were carried out on a rapid-scan, pulsed-lamp Varian Cary 50 spectrophotometer equipped with a fiber-optic dip probe (Varian Inc., Victoria, Australia). The probe (optical path 1 cm) was dipped into a 5 mL protein solution contained in a thermostated (20 °C) cylindrical cell together with the pH electrode (Radiometer, Copenhagen, Denmark). The protein solution was unbuffered in 0.1 M NaCl. A few microliters of NaOH or HCl solution (from 0.05 to 1 M) was added to the protein solution under stirring, and the visible spectrum and the pH value were recorded simultaneously. This procedure ensures the collection of a large number (20−50) of data points in a relatively short time (30 min). The data sets were analyzed in terms of a single pH-dependent transition for His69 → Val HbI and of two pH-dependent transitions for Phe97 → Leu HbI.

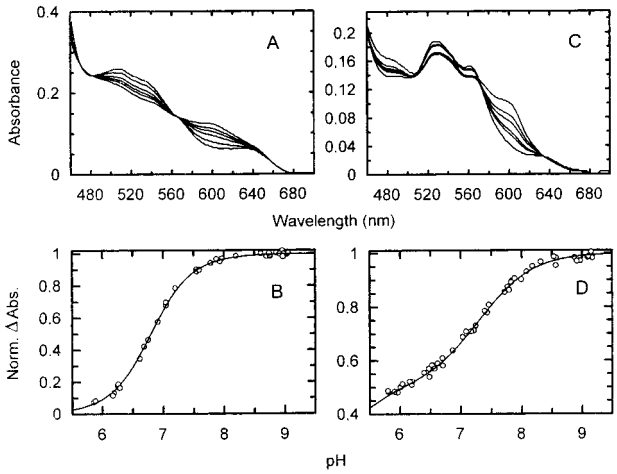

FIGURE 1: pH titrations of H69 → Val and Phe97 → Leu *S. inaequivalvis* hemoglobin mutants in the ferric state. Panels A and C shows the visible absorption spectra of H69 → Val and Phe97 → Leu HbI, respectively, as a function of pH, in unbuffered 0.1 M NaCl solutions, at 20 °C. pH values ranges from 5.8 to 9.0. For clarity, only a few spectra are presented. Panels B and D shows the titration profiles obtained for the two proteins together with the least-squares fitting curves (solid lines). A p*K* value of 6.8 ± 0.1 was obtained for H69 → Val HbI (panel B) and two p*K* values of 4.7 ± 0.2 and 7.2 ± 0.1 were obtained for Phe97 → Leu (panel D).

Resonance Raman spectra were measured on 40−60 μM protein solutions buffered with BisTris-HCl buffer, pH 5.8, $I = 0.1$ M, or with sodium tetraborate hydrochloride buffer, pH 8.5, $I = 0.1$ M, at 20 °C. The sample was irradiated with the 413.1 nm line of a krypton ion laser (Coherent Radiation Innova). The Raman signal was collected in the backscattering mode with a Labram spectrometer (Spex, Metuchen, NJ) equipped with a 1800 groove/cm grid, with a resolution of 2.5 cm^{-1}. The laser light was filtered with a super notch filter (Kaiser, Ann Harbor, MI).

Sedimentation velocity experiments were performed at 10 °C and 40 000 rpm on a Beckman Optima XL-A analytical ultracentrifuge equipped with absorbance optics. The protein concentration was in the range $(5-10) \times 10^{-5}$ M in BisTris-HCl buffer, pH 6.0, $I = 0.1$ M, and sodium tetraborate hydrochloride buffer, pH 8.5, $I = 0.1$ M. Data were collected at 530, 540, or 600 nm, depending on protein concentration and pH, at a spacing of 0.005 cm with three averages in a continuous scan mode and were analyzed with the program DCDT (*18*). The sedimentation coefficients were corrected to $s_{20,w}$ by standard procedures.

RESULTS

The pH dependence of the visible absorption spectra of His69 → Val HbI and Phe97 → Leu HbI is reported in Figure 1. In both mutants the spectral transition observed between pH 5.8 and 9.0 is reversible. In His69 → Val HbI, the spectral pattern as a function of pH shows clear isosbestic points, indicating that only two different spectral species are present at equilibrium (Figure 1, panel A). In contrast, in Phe97 → Leu HbI, the lack of isosbestic points indicates that more than two spectrally distinct species are present at equilibrium

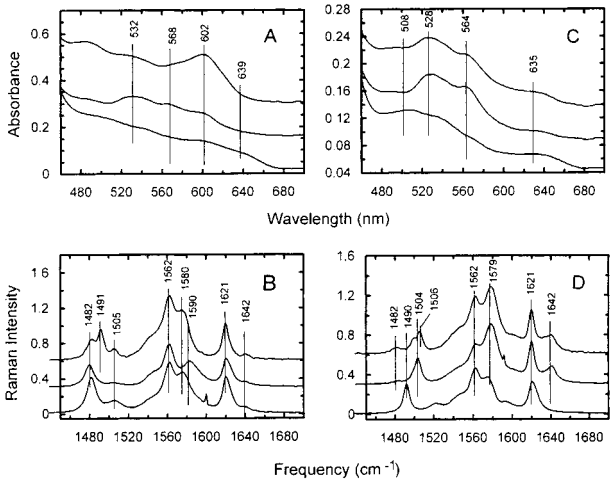

FIGURE 2: Visible absorption and resonance Raman spectra of H69 → Val and Phe97 → Leu *S. inaequivalvis* hemoglobin mutants in the ferric state. Panels A and B, from top to bottom: visible absorption (A) and resonance Raman (B) spectra of native, Phe97 → Leu and H69 → Val HbI at pH 8.5 in borate HCl (I = 0.1 M) buffer. Panels C and D, from top to bottom: visible absorption (C) and resonance Raman (D) spectra of native, Phe97 → Leu and H69 → Val HbI at pH 5.8 in Bis-Tris HCl (I = 0.1 M) buffer. Protein concentrations were 40−60 μM heme; temperature was 20 °C. Raman excitation wavelength was 413.1 nm, and laser power at the sample was 18 mW.

over the same pH range (Figure 1, panel C). The pH titrations have been fitted according to a single ionization step with a pK value of 6.8 in the case of His69 → Val (Figure 1, panel B) and with two ionization processes with pK values of 4.7 and 7.2, respectively, in Phe97 → Leu HbI (Figure 1, panel D).

The visible absorption spectra of ferric His69 → Val HbI and Phe97 → Leu HbI at acidic (pH = 5.8) and alkaline (pH = 8.5) pH values are compared in Figure 2 with the corresponding spectra of the native protein (top spectra in all panels). The absorption spectrum of the His69 → Val mutant (bottom spectra of Figure 2, panels A and C) displays the typical features of high-spin ferric hemes at both pH values. Thus, the broad high-spin marker band at ∼602 nm is the prominent feature at alkaline pH, while a high-spin band at 635 nm is apparent at acidic pH. The pH-dependent changes characterizing the Phe97 → Leu HbI spectra (middle spectra of Figure 2, panels A and C) are more complex. At low pH values, the absorption spectrum is indistinguishable from that of the native protein, i.e., is typical of a low-spin hemichrome, whereas at neutral and alkaline pH values the high-spin marker band at 602 nm is at the same wavelength as in the native protein but is of lower intensity.

The resonance Raman spectra add a further dimension to the observed spectral changes in both HbI mutants (Figure 2, panels B and D). The spin and coordination state marker bands that have been previously assigned in the native protein, namely ν_3, ν_2, and ν_{10} (*6*), can be readily identified in the mutated proteins. In the His69 → Val mutant at pH 5.8, ν_3 is at 1490 cm^{-1} and ν_2 at 1562 cm^{-1} (Figure 2, panel D, bottom spectrum). At alkaline pH values (Figure 2, panel B, bottom spectrum), ν_3 has a major component at 1482 and a minor band at 1505 cm^{-1}, while ν_2 is centered around 1562 cm^{-1}. At both pH values, ν_{10} probably overlaps with the vinyl mode at 1621 cm^{-1} although a small shoulder at 1642 cm^{-1} is also present at alkaline pH values.

The resonance Raman spectrum of the Phe97 → Leu mutant at acidic pH displays the ν_3 marker band at 1504 cm^{-1} and a small peak at about 1482 cm^{-1} (Figure 2, panel D, middle spectrum). At alkaline pH values, ν_3 displays a prominent feature at 1482 cm^{-1} and a minor component at 1505 cm^{-1} (Figure 2, panel B, middle spectrum). At pH 8.5, comparison of the Phe97 → Leu and native protein spectra brings out that the peak at 1491 cm^{-1}, characteristic of native HbI, is completely absent in the mutant. A small peak at 1642 cm^{-1} is found both in the native protein and in the mutant and can be attributed to the ν_{10} mode. Other features in the Raman spectrum, e.g., in the region 1560−1590 cm^{-1}, are more difficult to assign.

Sedimentation velocity experiments carried out at pH 6.0, 7.0, and 9.0 showed that the Phe97 → Leu mutant behaves like the native protein in that it is predominantly dimeric at alkaline pH values ($s_{20,w}$ = 2.5 S) and dissociates into monomers at low pH values ($s_{20,w}$ = 1.9 S). In contrast, the His69 → Val mutant is dimeric over the whole pH range ($s_{20,w}$ = 2.7−2.8 S).

DISCUSSION

The present study on the His69 → Val and Phe97 → Leu mutants of *Scapharca* HbI offers new insight into the structural constraints on the distal and proximal side of the heme pocket that are at the basis of the complex pH-dependent coordination and spin-state changes of the native ferric protein.

The coordination and spin state of the two mutants have been assigned by means of visible absorption and resonance Raman spectroscopy. Visible absorption spectroscopy provides a clear identification of the iron spin state, based upon the spectral analogies with a large number of hemoproteins and model compounds of known spin state (*1*, *2*). The presence of the iron d → heme π charge-transfer band at 602 or 635 nm is diagnostic of high-spin iron complexes. In turn, resonance Raman spectroscopy provides unique information on the heme iron coordination through the empirical correlations established between the frequencies of porphyrin core size modes and the iron coordination state. In particular, the frequencies relative to the ν_3, ν_2, and ν_{10} vibrational modes can be used to distinguish between five and six coordinate ferric hemes (*19*−*22*).

The visible absorption spectra of His69 → Val HbI indicate that the high-spin marker band at 602 nm is present at both low and high pH values together with a "high-spin"shoulder at 639 nm that increases upon decreasing pH. Hence, at variance with native HbI, the proton-driven high-spin to low-spin transition does not occur. The absence of the low-spin hemichrome species in the His69 → Val mutant at low pH provides further evidence that the distal His must furnish the sixth coordination bond to the ferric iron in native HbI (see Figure 3) (*6*). Resonance Raman spectroscopy of ferric His69 → Val HbI provides a clear assignment of the iron coordination states corresponding to the two high-spin species identified by visible absorption at low and high pH. The typical Raman coordination marker band, ν_3, is at 1482 cm^{-1} at alkaline pH values, as in five-coordinate high-spin species, but is centered at 1491 cm^{-1} at acidic pH values, as in hexacoordinate high-spin derivatives. The pH dependence of ferric His69 → Val HbI resembles that of *Aplysia* Mb

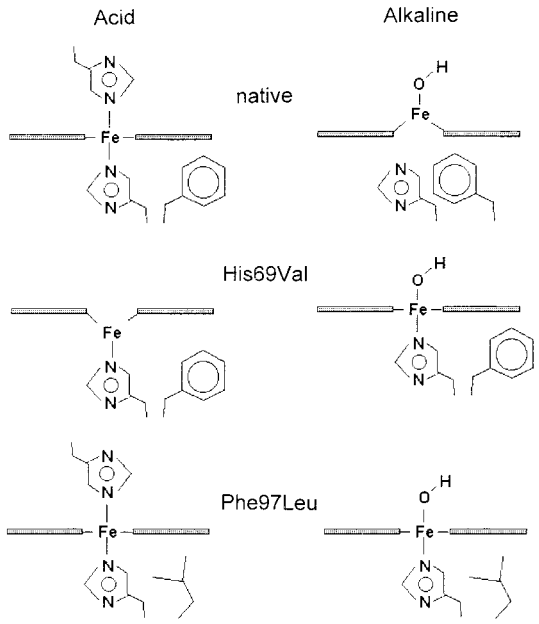

FIGURE 3: Modes of axial coordination in native, H69 → Val, and Phe97 → Leu *Scapharca* HbI in the ferric state at pH 5.8 (left side) and 8.5 (right side). In the native protein the proximal and distal histidine are shown together with the phenyl ring of Phe97 in its "R-like" (left) and "T-like" (right) position. In the H69 → Val mutant the phenyl ring stays in its "R-like" position; distal valine is not shown. In the Phe97 → Leu mutant, the Leu97 side chain is sketched next to the proximal histidine.

and "*Aplysia*-like" myoglobin mutants with a distal valine in that it is a single transition between two high-spin species with a p*K* around neutrality (*22*, *23*). According to the NMR studies of Qin et al. (*23*), ferric myoglobins coordinate water strongly only when there is a distal hydrogen-bond acceptor residue. Thus, the presence of an apolar residue in the distal side impairs binding of a water molecule to the heme iron both in *Aplysia* and in the His69 → Val mutant. In addition, Qin et al. (*23*) suggested that the hydroxide ion is coordinated strongly only in the presence of a distal hydrogen-bond donor, which was identified as ArgE10 in *Aplysia* Mb. In native and mutated *Scapharca* hemoglobins, such a hydrogen-bond donor cannot be postulated on the basis of the present data as well as from the crystallographic structures of the ferrous derivatives (*12*, *13*). Hence, the strength of the iron−hydroxyl link must originate from structural features other than distal hydrogen bonding. It is tempting to correlate the stability of the iron−hydroxyl complex to an "ionic couple effect", i.e., to the increased electrostatic interaction between the positively charged ferric ion and a negatively charged ligand due to the low polarity of the distal pocket. The same phenomenon was suggested to be responsible for the unusually high affinity of native HbI (both in the ferrous and ferric state) for the negatively charged cyanide anion (*24*) as well as for the formation of a stable iron−hydroxide bond in ferric hemin embedded in SDS micelles (*10*).

The spectroscopic data on the Phe97 → Leu mutant indicate that three distinct species participate to the observed pH-dependent profile. At low pH values, a low-spin hemichrome is formed as indicated by the features of the optical absorption (maximum at 532 nm, absence of high-spin marker bands) and resonance Raman (ν_3 at 1504 cm^{-1} and ν_{10} at 1642 cm^{-1}) spectra (Figure 1, panels B and D). This species is indistinguishable from that observed in the native protein. In contrast, at alkaline pH values, marked differences are observed in the resonance Raman spectrum of the Phe97 → Leu mutant with respect to the native protein. The ν_3 band at 1491 cm^{-1}, typical of a high-spin pentacoordinate derivative, is not present in the mutant which displays a clear peak at 1482 cm^{-1}, assigned to a high-spin hexacoordinate species, together with a broad peak at 1504 cm^{-1}, typical of a low-spin adduct (*19*−*22*). In line with the Raman data, the visible absorption spectrum of the Phe97 → Leu mutant at alkaline pH shows a large contribution from a high-spin species at 602 nm that is less intense than in the native protein. The alkaline spectrum of the Phe97 → Leu mutant is almost superimposable to that observed in horse Mb at pH 9.0. This similarity, taken together with the Raman spectral features, indicates that the alkaline Phe97 → Leu HbI is a mixture of water- and hydroxyl-bound hexacoordinate species. As in horse myoglobin, an increase in pH above 8.5 leads to a relative increase of hexacoordinate high-spin band (data not shown) (*25*).

The picture that emerges from the data on the Phe97 → Leu mutant is consistent with the proposed role of the Phe97 residue in the ferrous protein (*11*, *16*). It has been suggested that, at alkaline pH values, the phenyl ring of Phe97 is positioned within the proximal side of the heme pocket and exerts a packing strain on the proximal histidine just as in the deoxygenated derivative. In the ferric derivative, this strain leads to the cleavage of the proximal histidine iron bond and to formation of the unusual hydroxyl-bound pentacoordinate species (*1*). The leucine side chain, in the Phe97 → Leu mutant, though facing the proximal histidine, is unable to exert a strain on this residue, as reported by Pardanani et al. (*16*) in a crystallographic study on the deoxy ferrous derivative. It follows that the ferric high-spin Phe97 → Leu mutant, though frozen in "T-like" conformation, maintains the proximal histidine−iron bond (Figure 3). The behavior of the His69 → Val HbI completes the picture since it is a hexacoordinate high-spin species at alkaline pH even in the presence of the Phe97 side chain. This finding is consistent with the reported stabilization of this mutant in a "R-like" state (*15*), i.e., in a conformation with the Phe97 residue oriented toward the subunit interface (Figure 3).

A last point concerns the spin-state-linked association−dissociation equilibrium. In native HbI, dissociation into monomers has been correlated to the protonation of a heme carboxylate residue that is involved in a hydrogen bond with the Lys96 amino group on the contralateral subunit. In previous work, the p*K* values of 7−7.5 and 4.5−5 have been assigned to the protonation of the hydrogen-bonded (in the dimeric species) and free (in the monomer) heme carboxyl group, respectively (*5*, *6*). From a mechanistic point of view, dissociation into monomers was thought to precede the collapse of the heme pocket leading to the formation of a low-spin hemichrome. This mechanism is questioned by the present findings on His69 → Val HbI. As demonstrated by the analytical ultracentrifugation data, the mutated protein is dimeric and high-spin even at pH 6.0, suggesting that dissociation into monomers cannot be ascribed solely to the protonation of heme carboxyls. On the basis of the present data, in the native protein, the formation of a low-spin hemichrome must precede the dissociation step and is not the consequence of the collapse of the heme pocket after

monomer formation. It follows that protonation of carboxyls favors the collapse of the distal histidine over the iron atom. Dissociation into monomers, therefore, occurs as a result of a structural rearrangement of the interface, which is the direct consequence of the heme pocket collapse. At present, it is difficult to envisage the structural details of the spin-linked conformational changes that lead to subunit dissociation, and the solution of this problem should await the availability of X-ray quality crystals of the ferric protein.

ACKNOWLEDGMENT

We gratefully acknowledge Dr. Alberto Desantis for his help in the setup of the resonance Raman apparatus.

REFERENCES

1. Das, T. K., Boffi, A., Chiancone, E., and Rousseau, D. L. (1999) *J. Biol. Chem. 274*, 2916−2919.
2. Brancaccio, A., Cutruzzolà, F., Travaglini-Allocatelli, C., Brunori, M., Smerdon, S. J., Wilkinson, A. J., Dou, Y., Keenan, D., Ikeda-Saito, M., Brantley, R. E., Jr., and Olson, J. S. (1994) *J. Biol. Chem. 269*, 13843−13853.
3. Ikeda-Saito, M., Hori, H., Anderson, L. A, Prince, R. C., Pickering, I. J., George, G. N., Sanders, C. R., II, Lutz, R. S., McKelvey, E. J., and Mattera, R. (1992) *J. Biol. Chem. 267*, 22843−22852.
4. Spagnuolo, C., Ascoli, F., Chiancone, E., Vecchini, P., and Antonini, E. (1983) *J. Mol. Biol. 164*, 627−644.
5. Spagnuolo, C., De Martino, F., Boffi, A., Rousseau, D. L., and Chiancone, E. (1994) *J. Biol. Chem. 269*, 20441−20445.
6. Boffi, A., Takahashi, S., Spagnuolo, C., Rousseau, D. L., and Chiancone, E. (1994) *J. Biol. Chem. 269*, 20437−20440.
7. Salerno, J. C. and Leigh, J. S. (1984) *J. Am. Chem. Soc. 106*, 2156−2159.
8. Das, T. K., Franzen, S., Pond, A., Dawson, J. H., and Rousseau, D. L. (1999) *Inorg. Chem. 38*, 1952−1953.
9. Morikis, D., Champion, P. M., Springer, B. A., Egeberg, K. A., and Sligar S. G. (1990) *J. Biol. Chem. 265*, 12143−12145.
10. Boffi, A., Das, T. K., Della Longa, D., Spagnuolo, C., and Rousseau, D. L. (1999) *Biophys. J. 77*, 1143−1149.
11. Royer, W. E., Jr., Hendrickson, W. A., and Chiancone, E. (1989) *J. Biol. Chem. 264*, 21052−21061.
12. Royer, W. E., Jr., Hendrickson, W. A., and Chiancone, E. (1990) *Science 249*, 518−521.
13. Condon, P. J., and Royer, W. E., Jr. (1994) *J. Biol. Chem. 269*, 25259−25267.
14. Chiancone, E., Vecchini, P., Verzili, D., Ascoli, F., and Antonini, E. (1981) *J. Mol. Biol. 152*, 577−592.
15. Guarrera, L., Colotti, G., Boffi, A., Chiancone, E., Das, K. T., Rousseau, D. L., and Gibson, Q. H. (1998) *Biochemistry 37*, 5608−5615.
16. Pardanani, A., Gibson, Q. H., Colotti, G., and Royer, W. E., Jr. (1997) *J. Biol. Chem. 272*, 13171−13179.
17. Summerford, C. M., Pardanani, A., Betts, A. H., Poteete, A. R., Colotti, G., and Royer, W. E., Jr. (1995) *Protein Eng. 8*, 593−599.
18. Stafford, W. F. (1992) *Anal. Biochem. 203*, 295−301.
19. Hu, S., Smith, K. M., and Spiro, T. G. (1996) *J. Am. Chem. Soc. 118*, 12638−12646.
20. Feis, A., Marzocchi, M. P., Paoli, M., and Smulevich, G. (1994) *Biochemistry 33*, 4577−4583.
21. Rousseau, D. L., Ching, Y., Brunori, M., and Giacometti, G. M. (1989) *J. Biol. Chem. 264*, 7878−7881.
22. Giacometti, G. M., Ascenzi, P., Brunori, M., Rigatti, G., Giacometti, G., and Bolognesi. M. (1981). *J. Mol. Biol. 151*, 315−319.
23. Qin, J., Pande, U., La Mar, N. G., Ascoli, F., Ascenzi, P., Cutruzzolà, F., Travaglini-Allocatelli, C., and Brunori, M. (1993) *J. Biol. Chem. 268*, 24012−24021.
24. Boffi, A., Ilari, A., Spagnuolo, C., and Chiancone, E. (1996) *Biochemistry 35*, 8068−8074.
25. Antonini, E., and Brunori, M. (1971) in *Hemoglobin and Myoglobin in their Interactions with Ligands*, pp 40−53, North-Holland Publishing Co., Amsterdam, The Netherlands.

BI9923003